

# Best voltage bias-flipping strategy towards maximum piezoelectric power generation

Junrui Liang<sup>1</sup> and Henry Shu-Hung Chung<sup>2</sup>

<sup>1</sup> School of Information Science and Technology, ShanghaiTech University, 319 Yueyang Road, Shanghai 200031, China

<sup>2</sup> Centre for Smart Energy Conversion and Utilization Research, City University of Hong Kong, Kowloon Tong, Hong Kong, China

E-mail: liangjr@shanghaitech.edu.cn

**Abstract.** In piezoelectric energy harvesting (PEH) systems, energy extracted from piezoelectric structure can be increased by making piezoelectric voltage in phase with vibration velocity and raising the voltage amplitude. Such voltage manipulations can be realized by synchronously flipping the piezoelectric voltage with respect to a bias dc source at every displacement extremum. Given that net harvested energy is obtained by deducting dissipated energy from total extracted energy, a sophisticated voltage bias-flipping scheme, which can maximize extracted energy at low dissipative cost, is required towards harvested energy optimization. This paper extends the state of the art by proposing the best bias-flip strategy, which is delivered on conceptual synchronized multiple bias-flip (SMBF) interface circuits. The proposed strategy coordinates both requirements on larger voltage change in synchronized instant for more extracted energy and smaller voltage change in each bias-flip action for less dissipated energy. It not only leads to further enhancement of harvesting capability beyond existing solutions, but also provides an unprecedented physical insight on maximum achievable harvesting capability of PEH interface circuit.

## 1. Introduction

In piezoelectric energy harvesting (PEH), various harvesting interface circuits have been developed one after another, refreshing the record of harvesting capability [1]. Among these solutions, the synchronized switch harvesting on inductor (SSHI) has set a milestone in circuit development of PEH systems [2]. Recent development has shown that, compared to SSHI case, more energy might be rewarded by subtly returning a part of the reclaimed energy to the vibrating structure at right moments. Such solutions were called energy injection [3], pre-biasing [4], or energy investment [5]. The control of energy flow in these solutions is achieved by successively flipping the voltage across piezoelectric element twice through two different bias dc voltages: one for harvesting energy, called *passive* bias-flip action in this paper; and the other for investing energy, called *active* bias-flip action. Given the seemingly endless development trend of PEH interface circuit, it is curious that:

- whether PEH capability can go beyond the state-of-the-art solutions?
- which kind of solution yields the best PEH capability, passive or hybrid (passive + active)?
- whether PEH capability in the latest double bias-flip solutions has already been optimized?
- is there any limit for the improvement of PEH interface circuit?



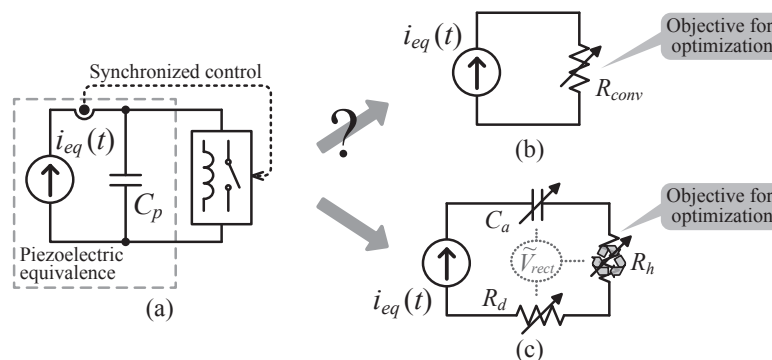


**Figure 1.** Bias-flip solution for PEH. (a) Principle. (b) Equivalence targeted at power conversion (extraction). (c) Equivalence targeted at energy harvesting [11].

Inspired by these curiosities, this paper generalizes the state-of-the-art bias-flip solutions with a conceptual synchronized multiple bias-flip (SMBF) circuit topology. The best voltage bias-flipping strategy towards maximum PEH capability is then developed based on this generalized SMBF topology. Through these theoretical development, new insights are gained for better understanding and further improvement of PEH interface circuit [3, 4, 5].

## 2. Objective for PEH optimization

The bias-flip technique was originally developed to enhance piezoelectric conversion for vibration damping purpose [6, 7]. Its principle is shown in figure 1(a). By synchronously flipping the piezoelectric voltage with respect to zero [6] or a bias dc voltage source [7] at zero-crossing instants of vibration velocity, the combination of piezoelectric capacitance  $C_p$  and connected circuit might behave like a tunable resistance  $R_{conv}$ , as shown in figure 1(b). Given the correlation between energy harvesting and vibration damping [8], the increase of electrically induced damping was once regarded as target for PEH circuit improvement in some studies [8, 9]. Yet, distinguishing the effects between harvested energy and dissipated energy (unavoidable during power conditioning) in total extracted energy, only the harvested portion should be identified as objective for PEH [10], as shown in figure 1(c). Therefore, exactly speaking, PEH circuit improvement should be specified to maximize the electrically induced damping *at low dissipative cost*. Synchronously inverting the piezoelectric voltage through an inductor provides the possibility towards this goal [2, 3, 4, 5].

## 3. SMBF interface circuits

From energy cycle analysis [10], given a PEH system vibrating with constant amplitude, more extracted energy requires larger voltage change before and after voltage flipping state; on the other hand, less dissipated energy requires smaller voltage change before and after each bias-flip action, because dissipated energy in a bias-flip action *parabolically rise* with such voltage change. The only way to satisfy both requirements is to make a large voltage change by combining multiple small steps, which leads to the proposal of SMBF interface circuits.

The circuit topologies of SMBF are shown in figure 2. The two configurations of series SMBF (S-SMBF) and parallel SMBF (P-SMBF) are quite similar to S-SSHI and P-SSHI, respectively, except that there are multiple bias dc sources for continuous bias-flip actions. In every zero-crossing instant of  $i_{eq}$ , the piezoelectric voltage  $v_p$  are flipped for  $M$  times with respect to the bias dc sources from  $V_{b,1}$ ,  $V_{b,2}$  to  $V_{b,M}$  in sequence. These bias voltages are assumed unknown variables at start; source symbols in figure 2 are only for indicating positive directions. Half of the switch paths with switch  $S_{+m}$  are for positive current flippings, while the others with switch

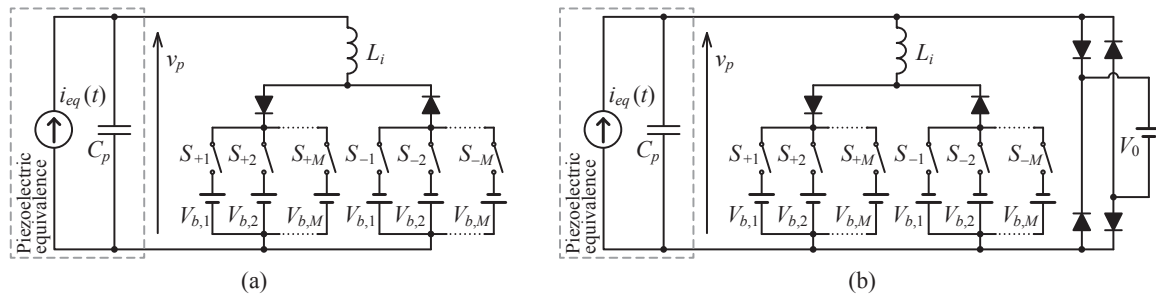


**Figure 2.** Conceptual SMBF interface circuits. (a) S-SMBF. (b) P-SMBF.

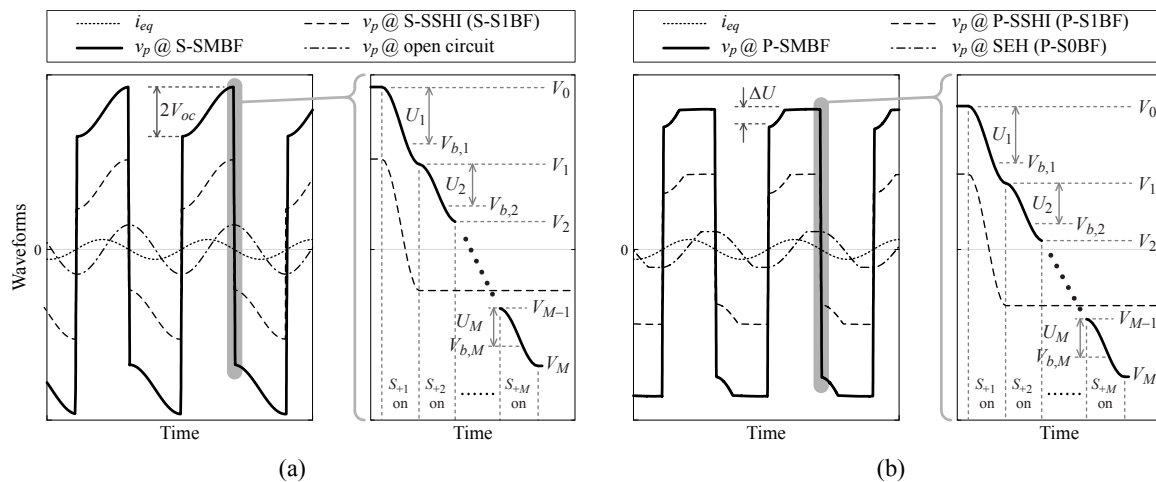


**Figure 3.** Waveforms in SMBF. (a) S-SMBF. (b) P-SMBF.

$S_{-m}$  are for negative ones. Each switch-on time is half of an  $LC$  cycle, i.e.,  $\pi\sqrt{L_i C_p}$ , for making largest voltage change with lowest dissipative cost. Therefore, flipping factor  $\gamma = -e^{-\pi/(2Q)}$ .

Figure 3 shows the waveforms in SMBF. Compared to conventional SSHI, SMBF can further boost the amplitude of  $v_p$ , which implies that more power can be extracted from the piezoelectric structure. In fact, S-SSHI can be regarded as S-S1BF (special case of S-SMBF with  $M = 1$ ); P-SSHI and standard energy harvesting (SEH) interface can be regarded as P-S1BF and P-S0BF (special cases of P-SMBF with  $M = 1$  and  $0$ ), respectively. The switch schedule in a synchronized instant is also zoomed in and shown in figure 3. The intermediate voltages in an SMBF process are denoted as  $V_m$  ( $m = 0, 1, 2, \dots, M$ ); their differences to the bias voltages  $V_{b,m+1}$  are denoted as  $U_{m+1}$ .

#### 4. Best voltage bias-flipping strategy

The advancement of SMBF on piezoelectric power generation needs to be mathematically justified. With the denotations about intermediate voltages of  $v_p$  and bias dc sources, which were given in figure 3, voltage relations among these unknown voltages in all SMBF solutions are summarized by (1). Regarding all voltages are nondimensionalized with respect to the open circuit voltage  $V_{oc}$ ; and nondimensionalizing all energy amounts with respect to  $C_p V_{oc}^2$ , maximum harvestable energy in one cycle by using SEH, the net total energy income of all bias dc sources in figure 2 is given by (2), where each  $V_{b,m}$  can be expressed as functions of  $U_1, U_2, \dots, U_M$ , and  $\Delta U$ . Since  $U_1, U_2, \dots, U_M$ , and  $\Delta U$  are independent variables, optimal harvesting condition can be obtained by solving (3), where  $m = 1, 2, \dots, M$ . In P-SMBF, all  $U_m$  and  $\Delta U$  can be

$$\begin{bmatrix} 1 & & & & & & 1 \\ 1 & -1 & & & & & \\ & & \ddots & \ddots & & & \\ & & & 1 & -1 & & \\ & & & & \ddots & \ddots & \\ & & & & & 1 & -1 \end{bmatrix} \begin{bmatrix} V_0 \\ V_1 \\ \vdots \\ V_m \\ \vdots \\ V_M \end{bmatrix} = \begin{bmatrix} \Delta U \\ (1-\gamma)U_1 \\ \vdots \\ (1-\gamma)U_m \\ \vdots \\ (1-\gamma)U_M \end{bmatrix} \quad (1)$$

$$E_h = 2 \left[ \sum_{m=1}^M (1-\gamma) U_m V_{b,m} + (2 - \Delta U) V_0 \right] \quad (2)$$

$$\begin{cases} \frac{\partial E_h}{\partial U_m} = 0 \\ \frac{\partial E_h}{\partial \Delta U} = 0 \end{cases} \Rightarrow \begin{cases} U_{m,opt} = \frac{1}{1+\gamma} \\ \Delta U_{opt} = 1 \end{cases} \quad (3)$$

$$(E_{h,max})_{\text{P-SMBF}} = M \frac{1-\gamma}{1+\gamma} + 1; \quad (E_{h,max})_{\text{S-SMBF}} = M \frac{1-\gamma}{1+\gamma} \quad (4)$$

$$(E_{h,max})_{\text{SSPB}} = -\frac{8\gamma}{1+\gamma^2} \quad (5)$$

tuned for approaching this optimal harvesting condition; while in S-SMBF,  $\Delta U$  is fixed at 2. Under optimal harvesting condition, maximum harvested energies in both cases are derived as (4). The purpose of energy injection [3], pre-biasing [4], and energy investment [5] is to achieve the S-S2BF case. Yet, in these previous solutions, the intermediate voltage  $V_1$  is mandatorily fixed at zero, rather regarded as free for optimization. In the single-supply pre-biasing (SSPB) solution [4], maximum harvested energy is given by (5).

Based on (4) and (5), figure 4(a) illustrates the nondimensional maximum harvested energy as function of  $\gamma$  in optimal P-, S-SMBF, and SSPB. It shows that, under the same bias-flip number  $M$ , optimal P-SMBF is able to harvest more energy than its series counterpart. All  $E_{h,max}$  approach infinity as  $\gamma$  approaches  $-1$  (ideal lossless flipping case), except the  $M = 0$  cases. The larger  $M$ , i.e., more bias-flip actions for  $v_p$  in each synchronized instant, the larger  $E_{h,max}$  under same  $\gamma$ . For SSPB, as observed from figure 4(a), it outperforms optimal SEH (P-S0BF), S-SSHI (S-S1BF), and P-SSHI (P-S1BF) when  $\gamma < -0.123$ ,  $-0.172$ , and  $-0.333$ , respectively. Yet, it cannot catch up with optimal S-S2BF, whose circuit topology and operation are the same, except  $V_1$  is free rather than fixed in optimization. Figure 4(b) shows the maximum harvested energy  $E_{h,max}$  as function of  $V_1$  in general S-S2BF configuration. Simulation results obtained with PSIM software show good agreement with theoretical prediction. More energy can be harvested when  $V_1 = 1$  rather than 0, regardless of  $\gamma$ . Therefore, rather than presuming any intermediate voltages, equation (3) should be regarded as a guideline towards maximum energy harvesting capability for SMBF interface circuits.

## 5. Conclusion

This paper has discussed some crucial questions towards better understanding and future development of piezoelectric energy harvesting (PEH) interface circuit. Through the theory development, it is found that:

- a) PEH capability might exceed state-of-the-art solutions by involving more bias-flip actions in every synchronized instant;

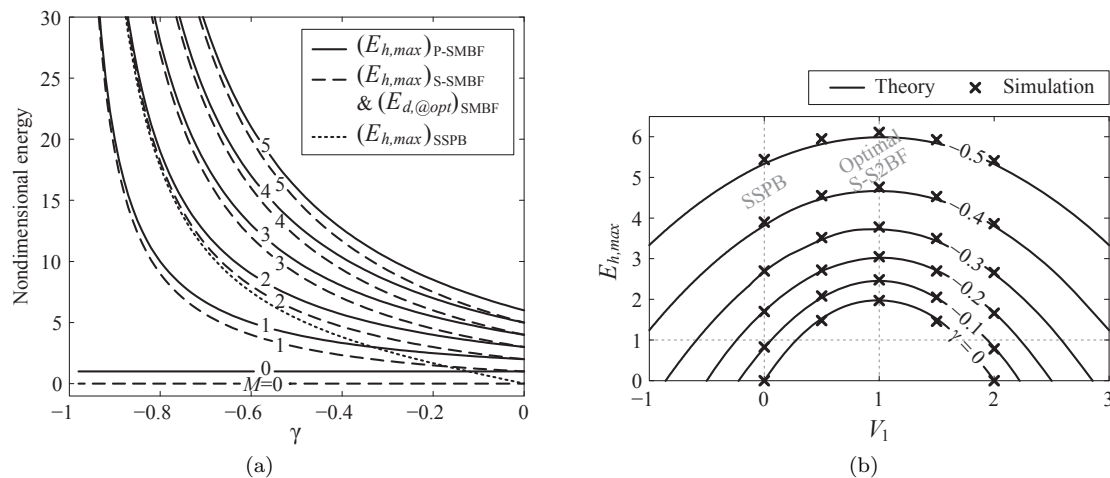


**Figure 4.** Maximum harvested energy in (a) different solutions, (b) S-S2BF under different intermediate voltage  $V_1$ .

- b) for flipping number  $M < 2$ , passive bias-flip solutions give better harvesting capability, while for  $M \geq 2$ , hybrid solutions perform better;
- c) harvested power in the latest S-S2BF solutions can be further optimized by adjusting the intermediate voltage;
- d) under constant amplitude vibration, harvested power might approach infinity by either decreasing the inversion factor  $\gamma$  or increasing the flipping number  $M$  in SMBF; yet, under force excitation, it is confined by mechanical dynamics.

Given the rational guidance provided by the proposed strategy, more efforts should be taken on multi-source implementation, switches management, etc. towards technical realization of SMBF circuits and the best harvesting strategy delivered on them.

## References

- [1] Szarka G D, Stark B H and Burrow S G 2012 Review of power conditioning for kinetic energy harvesting systems *IEEE Trans. Power Electron.* **27** 803–815
- [2] Guyomar D, Badel A, Lefeuvre E and Richard C 2005 Toward energy harvesting using active materials and conversion improvement by nonlinear processing *IEEE Trans. Ultrason. Ferroelectr. Freq. Control* **52** 584–595
- [3] Lallart M and Guyomar D 2010 Piezoelectric conversion and energy harvesting enhancement by initial energy injection *Appl. Phys. Lett.* **97** 014104 (pages 3)
- [4] Dicken J, Mitcheson P, Stoianov I and Yeatman E 2012 Power-extraction circuits for piezoelectric energy harvesters in miniature and low-power applications *IEEE Trans. Power Electron.* **27** 4514–4529
- [5] Kwon D and Rincon-Mora G A 2012 Energy-investment schemes for increasing output power in piezoelectric harvesters *IEEE 55th International Midwest Symposium on Circuits and Systems* pp 1084–1087
- [6] Richard C, Guyomar D, Audigier D and Ching G 1999 Semi-passive damping using continuous switching of a piezoelectric device *Smart Structures and Materials 1999: Passive Damping and Isolation* vol 3672 (SPIE) pp 104–111
- [7] Ji H, Qiu J, Adrien B and Zhu K 2009 Semi-active vibration control of a composite beam using an adaptive ssdv approach *J. Intell. Mater. Syst. Struct.* 401–412
- [8] Wang Y and Inman D J 2012 A survey of control strategies for simultaneous vibration suppression and energy harvesting via piezoceramics *J. Intell. Mater. Syst. Struct.* **23** 2021–2037
- [9] Miller L M, Mitcheson P D, Halvorsen E and Wright P K 2012 Coulomb-damped resonant generators using piezoelectric transduction *Appl. Phys. Lett.* **100** 233901 (pages 4)
- [10] Liang J R and Liao W H 2011 Energy flow in piezoelectric energy harvesting systems *Smart Mater. Struct.* **20** 015005
- [11] Liang J R and Liao W H 2012 Impedance modeling and analysis for piezoelectric energy harvesting systems *IEEE/ASME Trans. Mechatron.* **17** 1145–1157